

Grain carbon isotope composition is a marker for allocation and harvest index in wheat

Jean-Baptiste Domergue¹, Cyril Abadie¹, Julie Lalande¹, Jean-Charles Deswarte², Eric Ober³, Valérie Laurent⁴, Céline Zimmerli⁵, Philippe Lerebour⁶, Laure Duchalais⁷, Camille Bédard⁸, Jérémy Derory⁹, Thierry Moittie¹⁰, Marlène Lamothe-Sibold¹¹, Katia Beauchêne¹², Anis M. Limami¹ & Guillaume Tcherkez^{1,13*}

1. Institut de Recherche en Horticulture et Semences, Université d'Angers, INRAe, 42 rue Georges Morel, 49071 Beaucouzé, France.
2. Arvalis Institut du Végétal, Pôle valorisation de l'écophysiologie, ZA des Gravieres, 91190 Villiers le Bâcle, France.
3. National Institute of Agricultural Botany, 93 Lawrence Weaver Road, Cambridge, CB3 0LE, United Kingdom.
4. Florimond Desprez Veuve et fils, BP 41, 59242 Cappelle-en-Pévèle, France.
5. BASF France S.A.S., La Ferme du Paly, 91490 Milly-la-Forêt, France.
6. Unisigma, GIE Recherche et Création Variétale, 2 rue Petit-Sorri, 60480 Froissy, France.
7. RAGT 2n, Route Epincy, 28150 Louville-la-Chenard, France.
8. Secobra Recherches, Centre de Bois-Henry, 78580 Maule, France.
9. Limagrain Europe, Centre de recherche, CS 50005, Saint Beauzire, 63360 Gerzat, France.
10. ASUR Plant Breeding, 163 ter avenue de Flandre, 60190 Estrées-Saint-Denis, France.
11. SPOMics plant métabolisme métabolome platform, Institute of Plant Sciences Paris-Saclay IPS2, CNRS, INRAe, Universities Paris-Saclay, Evry and Paris, Batiment 630, 91405 Orsay, France.
12. Arvalis Institut du Végétal, Pôle PhenoHD3, 45 voie Romaine, Ouzouer-le-Marché, 41240 Beauce-La-Romaine, France.
13. Research School of Biology, ANU College of Science, Australian National University, 2601 Canberra ACT, Australia.

*Contact author to whom correspondence should be addressed

Email: guillaume.tcherkez@anu.edu.au

Word count (w/o references): 4,966

Keywords: wheat, isotope, carbon 13, harvest index, respiration use efficiency

1 **Abstract** (222 words)

2 The natural ^{13}C abundance ($\delta^{13}\text{C}$) in plant leaves has been used for decades with great
3 success in agronomy to monitor water use efficiency and select modern cultivars adapted
4 to dry conditions. However, in wheat, breeding also implies looking for genotypes with
5 high carbon allocation to spikes and grains, and thus with a high harvest index and/or low
6 carbon losses via respiration. Finding isotope-based markers of optimal carbon
7 partitioning to grains would be extremely useful since isotope analyses are inexpensive
8 and can be performed routinely at high throughput. Here, we took advantage of a set of
9 field trials made of more than 600 plots with several wheat cultivars and measured
10 agronomic parameters as well as $\delta^{13}\text{C}$ values in leaves and grains. We find a linear
11 relationship between the apparent isotope discrimination between leaves and grain
12 (denoted as $\Delta\delta_{\text{corr}}$), and the respiration use efficiency-to-harvest index ratio. It means that
13 overall, efficient carbon allocation to grains is associated with a small isotopic difference
14 between leaves and grains. This effect is explained by post-photosynthetic isotope
15 fractionations, and we show that this can be rationalised by equations describing the
16 carbon isotope composition in grains along the wheat growth cycle. Our results thus show
17 that ^{13}C natural abundance in grains has some potential to help finding genotypes with
18 better carbon allocation properties and assisting current wheat breeding technologies.

19 **Introduction**

20 The quantitation of stable carbon isotopes (^{12}C , ^{13}C) is currently a major technology for
21 crop cultivar selection and authentication of food products, representing a huge market in
22 fraud detection and quality assessment (Kelly *et al.*, 2005). In particular, the natural ^{13}C
23 abundance (or isotope composition, $\delta^{13}\text{C}$) is used routinely to probe photosynthetic
24 pathways (C_3 , C_4 , CAM) and thereby certify the origin of many food products consumed
25 worldwide, such as flavours (Remaud & Akoka, 2017) (e.g., vanillin) and beverages
26 (Santesteban *et al.*, 2015) (e.g., wine). In C_3 plants like wheat, the natural isotope
27 composition in plant organic matter is ^{13}C -depleted by *c.* 20‰ compared to atmospheric
28 CO_2 while C_4 plants are ^{13}C -depleted by *c.* 4‰ only.

29 In C_3 crops, $\delta^{13}\text{C}$ is crucial to screen water-efficient cultivars by taking advantage
30 of the linear relationship between the isotope discrimination during photosynthesis (Δ)
31 and water use efficiency (WUE) (Condon *et al.*, 1987; Condon *et al.*, 1990; Condon *et al.*,
32 2004). Photosynthetic isotope discrimination essentially comes from two main steps:
33 First, the strong isotope effect (29‰) associated with CO_2 fixation catalysed by ribulose
34 1,5-bisphosphate carboxylase/oxygenase (Rubisco); Second, the small isotope effect
35 (4.4‰) by CO_2 diffusion from the atmosphere to leaf mesophyll cells (Farquhar *et al.*,
36 1989). It has also been demonstrated recently that internal conductance of CO_2 (from
37 intercellular spaces to chloroplasts) also affects significantly the estimation of intrinsic
38 WUE (iWUE) from carbon isotopes (Ma *et al.*, 2020). In water-efficient cultivars, the
39 generally lower stomatal conductance and/or higher photosynthetic capacity are so that
40 CO_2 diffusion is relatively more limiting and thus the isotope discrimination Δ is low,
41 causing a general ^{13}C -enrichment in plant matter. As a result, the $\delta^{13}\text{C}$ value in vegetative
42 material (typically flag leaf in wheat) directly reflects leaf photosynthetic properties and
43 can thus be used as a biomarker to find cultivars with high WUE values (Condon *et al.*,
44 2004). This technique has been widely and successfully implemented in wheat and other
45 species since the eighties because $^{13}\text{C}/^{12}\text{C}$ analyses are rapid and inexpensive using
46 current elemental analysis/mass spectrometry devices (Sanchez-Bragado *et al.*, 2020).

47 Nevertheless, although leaf $\delta^{13}\text{C}$ reflects photosynthetic performance and
48 associated water usage, it does not provide information on other parameters that are
49 essential for yield (Y) such as the harvest index (HI). In wheat, high-performing cultivars
50 are generally associated with higher tiller number, a high grain number per spike, and
51 relatively high HI (Sinclair, 1998; Reynolds *et al.*, 2012; Quintero *et al.*, 2018). In other
52 words, grain properties and carbon allocation to grains is a fundamental aspect of wheat
53 breeding that cannot be accounted for with current $\delta^{13}\text{C}$ analyses in vegetative material.
54 The question thus arises as to whether the isotope signature of grains, which are readily
55 amenable for biochemical analyses and cultivar ranking unlike fastidious and expensive
56 flag leaf sampling at anthesis, can be used to gain direct information on Y or HI. About
57 20 years ago, relationship was found between Y or HI and grain $\delta^{13}\text{C}$ ($\delta^{13}\text{C}_{\text{grain}}$) but this

58 was mostly driven by changes in iWUE, i.e., stomatal conductance and photosynthetic
59 capacity (Merah *et al.*, 2001a; Merah *et al.*, 2001b; Merah *et al.*, 2002). Whether $\delta^{13}\text{C}_{\text{grain}}$
60 can be exploited further to give access to agronomic parameters other than photosynthesis
61 or WUE has never been addressed.

62 In particular, variations in $\delta^{13}\text{C}_{\text{grain}}$ can be anticipated because of metabolic
63 isotope discriminations in grain biomass synthesis and/or respiratory CO_2 loss (so-called
64 "post-photosynthetic" isotope fractionations). Post-photosynthetic fractionations are
65 generally so that heterotrophic organs are ^{13}C -depleted compared to leaves (Badeck *et al.*,
66 2005; Cernusak *et al.*, 2009). In addition, there is an isotope discrimination during
67 metabolic decarboxylation and respired CO_2 is often naturally ^{13}C -enriched in leaves and
68 ^{13}C -depleted in heterotrophic organs (Bathellier *et al.*, 2017). Conversely, vegetative
69 plant organic matter is mostly made of cellulose, which is generally ^{13}C -enriched
70 compared to photosynthetically fixed carbon (Gleixner *et al.*, 1993; Schmidt & Gleixner,
71 1998; Kodina, 2010). At the metabolic scale, it has been shown that the intramolecular
72 ^{13}C distribution ($\delta^{13}\text{C}$ values at the different C-atom positions) in wheat grain starch is
73 dictated by isotope effects in metabolism and partitioning between starch production and
74 glycolysis (Gilbert *et al.*, 2012). Similarly, at the plant scale, variations in carbon
75 partitioning to grains at the expense of respiratory CO_2 loss or vegetative organic matter
76 likely cause changes in $\delta^{13}\text{C}_{\text{grain}}$ due to isotopic mass-balance.

77 Here, we exploited a dataset of $\delta^{13}\text{C}$ values and agronomic variables (such as
78 biomass, N content, yield, grain weight, consumed water, etc.) obtained in winter wheat
79 grown in the field, across different sites (Table 1 and Fig. S1), representing a total of 644
80 field plots and 70 cultivars. We also developed new equations describing the isotope
81 composition in grains as a function of carbon allocation parameters, HI or Y. We find
82 that the leaf-to-grain carbon isotope discrimination relates to the respiration use
83 efficiency-to-HI ratio. The observed relationship depends on neither the cultivation site
84 nor irrigation and thus offers good potential for allocation-based cultivar selection using
85 $\delta^{13}\text{C}_{\text{grain}}$ values.

86 **Material and methods**

87

88 *Cultivation*

89 Three series of randomized block field experiments (Fig. S1 and Table 1) were
90 undertaken at different locations, with different cultivars and varying water availability,
91 irrigated to maximal evapotranspiration, and non-irrigated (rainfed). Experiments
92 followed cultivation of wheat or other crops (sunflower, pea, rapeseed) as mentioned in
93 figures, on calcareous or clay substratum depending on the site considered. Crop
94 development was typical of French climatic regions with sowing in October-November,
95 seedling establishment in November, visible stem extension (growth stage Z30) at the
96 end of March or beginning of April, anthesis at the end of May and harvest maturity in
97 July.

98

99 *Measurement of agronomic parameters*

100 Experimental plots measured between 6 and 12 m² across experimental sites. Destructive
101 measurements (above-ground biomass and nitrogen content at Z30, Z65 and maturity,
102 leaf sampling at anthesis) were performed on a dedicated additional plot in each block,
103 with 2-3 biological replicates per plot. Non-destructive measurements (plant and spike
104 density at heading (Z55) and anthesis (Z65)) were carried out using the plot dedicated to
105 final harvest. Final yield was measured at the plot level using an experimental combine.
106 Grain parameters were measured as in (Touzy *et al.*, 2019). Grain samples from the
107 combine harvester was used to measure plot grain weight, grain humidity at harvest,
108 grain protein content, specific weight. Grain yield, grain number per m², grain number
109 per spike and grain weight per spike were calculated. At Saint-Pierre d'Amilly (VAR
110 site), actual soil water content was measured at Z30, Z65 and harvest using a soil neutron
111 probe (at 1.8-m depth) and water content variations between measurement dates were
112 used to monitor crop water consumption. At other sites (BPA, BVG), water balance was
113 followed using soil properties, meteorological data and actual irrigation when applicable.

114

115 *Isotopic analyses*

116 Isotopic analyses were done using oven-dry material ground in fine power and weighted
117 in tin (¹³C) or silver (¹⁸O) capsules. Samples were analysed using an isotope ratio mass
118 spectrometer Isoprime (Elementar, France) coupled to an elemental analyser (Carlo-Erba,
119 Italy) run in combustion (¹³C) or pyrolysis (¹⁸O). Delta value accuracy was checked using
120 IEAE standards USGS-40 (glutamic acid) and IAEA-CH7 (polyethylene) and IAEA-602
121 (benzoic acid) (¹³C) and ANU sucrose (home standard) (¹⁸O) every 10 samples. Isotopic
122 analyses were carried out by facilities Plateforme Métabolisme Métabolome (France) and
123 ANU Stable Isotope Laboratory (Australia). Delta values are expressed with respect to V-
124 PDB (¹³C) and V-SMOW (¹⁸O), in ‰. Climatic parameters used for computations

125 (temperature) was from Meteo France stations. $\delta^{18}\text{O}$ values in precipitation in the regions
 126 considered are from the database Nucleus (IAEA).

127

128 *Theory and calculations*

129

130 *Notations and assumptions.* The isotope composition ($\delta^{13}\text{C}$ value) is denoted as δ . Second
 131 order terms are neglected and thus, if the isotope fractionation of a given biochemical
 132 process is denoted as Δ then the isotope composition of the product δ_{product} is equal to
 133 $\delta_{\text{substrate}} - \Delta$. Symbols associated with carbon amounts are illustrated in Fig. S2. The
 134 decomposition in carbon flow and three different stages (pre-anthesis, early grain filling,
 135 late grain filling) in Fig. S2 is from model III in (Gent, 1994). Symbols associated with
 136 isotope compositions and fractionations are listed in Table S1. The term “isotope
 137 fractionation” refers to the change in delta value related to the observed isotope effect IE
 138 ($^{12}\text{C}/^{13}\text{C}$ ratio of velocity) as follows: fractionation = IE – 1. That way, the fractionation is
 139 positive when against the heavy (^{13}C) isotope. Here, for simplicity, we assumed that
 140 fractionations associated with reserve establishment (p_r), respiration (e_g , e_m) and grain
 141 biomass synthesis (β) did not vary between stages. We also neglect denominators ($\delta + 1$)
 142 which are assumed to be equal to unity (that is, we neglect second-order terms, see
 143 above).

144

145 *Flux mass balance.* Carbon balance is applied to C amounts as follows:

146 Stage 1: $A_1 = V_{r1} + V_s + R_{g1}$ and $V_{r1} = B_1 + R_{m1}$ (1)

147 Stage 2: $A_2 = V_{r2} + G + R_{g2}$ and $V_{r2} = B_2 + g_2 + R_{m2}$ (2)

148 Stage 3: $A_3 = V_{r3} + R_{g3}$ and $V_{r3} + B_3 = g_3 + R_{m3}$ (3)

149

150 *Harvest index.* The harvest index (HI) is defined as the ratio of grain biomass to total net
 151 biomass, which gives, using amounts of carbon:

152
$$\text{HI} = \frac{\text{grain carbon}}{\text{net total carbon}} = \frac{\Sigma g}{\Sigma A - \Sigma R_g - \Sigma R_m} = \frac{\Sigma g}{V_s + \Delta B + \Sigma g}$$
 (4)

153 where $\Sigma g = G + g_2 + g_3$, $\Sigma A = A_1 + A_2 + A_3$, $\Sigma R_g = R_{g1} + R_{g2} + R_{g3}$, $\Sigma R_m = R_{m1} + R_{m2} +$
 154 R_{m3} , and $\Delta B = B_1 + B_2 - B_3$. In principle, carbon remobilization is so that $\Delta B \approx 0$, that is,
 155 $B_1 + B_2 = B_3$. This assumption will be used here. Also, V_s and Σg are given by straw and
 156 grain carbon amounts, respectively.

157

158 *Isotopic mass balance.* The isotopic composition of photosynthetically fixed carbon (δ_{fix})
 159 must be equal to the weighted average of isotopic compositions of sink compartments
 160 (which account for fractionations) and thus, at stage 1:

161

162
$$A_1 \delta_{\text{fix}1} = V_{r1}(\delta_{\text{fix}1} - p_r) + V_s(\delta_{\text{fix}1} - p_s) + R_{g1}(\delta_{\text{fix}1} - e_g)$$
 (5)

163

164 where p_r , p_s and e_g is the isotope fractionation associated with reserves establishment,
165 structural biomass construction and growth respiration, respectively. Similarly, isotopic
166 mass balance on metabolism leads to:

167

$$168 \quad V_1(\delta_{\text{fix}1} - p_r) = B_1\delta_{B1} + R_{m1}(\delta_{B1} - e_m) \quad (6)$$

169

170 By substitution, the isotope composition of the metabolic reserve pool, δ_{B1} , can be
171 calculated as:

$$172 \quad \delta_{B1} = \frac{V_1(\delta_{\text{fix}1} - p_r) + R_{m1}e_m}{B_1 + R_{m1}} \quad (7)$$

173 The same procedure was applied to stages 2 and 3. For stage 2, it leads to:

$$174 \quad \delta_{B2} = \frac{V_2(\delta_{\text{fix}2} - p_r) + g_2\beta + R_{m2}e_m}{B_2 + g_2 + R_{m2}} \quad (8)$$

175 In stage 3, we have:

$$176 \quad \delta_{B3} = \frac{V_3(\delta_{\text{fix}3} - p_r) + B_3\delta_{B2} + g_3\beta + R_{m3}e_m}{g_3 + R_{m3}} \quad (9)$$

177 where β is the isotope fractionation during grain biomass synthesis. While there is some
178 variations depending on the organ considered, CO_2 respired by heterotrophic organs is
179 generally ^{13}C -depleted (Ghashghaie & Badeck, 2014; Bathellier *et al.*, 2017) and thus
180 across the full wheat life cycle, overall respiratory fractionation (e_{mg} used thereafter) is
181 likely positive and different scenarios (from 2.5 to 4‰) are shown in Fig. 4 in main text.
182 In our study, the fact that $e_g > 0$ is further supported by the fact that grains are ^{13}C -
183 enriched, in agreement with the possible difference in sign between β and e_g when V_{r2}/V_{r3}
184 is small (equation 13 below). The isotope fractionation in structural biomass synthesis is
185 negative (favours ^{13}C) due to the fact that straw is cellulose-rich and cellulose is naturally
186 ^{13}C -enriched. In wheat, it has been shown that straw and straw cellulose is ^{13}C -enriched
187 by up to 3‰ compared to flag leaf at anthesis (Merah *et al.*, 2002; Kodina, 2010). In
188 numerical applications, we thus used $p_s = -3‰$.

189

190 By definition, the isotope composition in grains is the weighted average of contributions
191 of the different sources, and therefore:

$$192 \quad \delta_{\text{grain}} = \frac{g_2\delta_{B2} + g_3\delta_{B3} + G\delta_{\text{fix}2} - \beta}{g_3 + g_2 + G} \quad (10)$$

193 Substituting (7), (8) and (9) in (10) gives:

$$\begin{aligned}
\delta_{\text{grain}} = & \frac{g_2 + g_3\varphi}{\Sigma g} \cdot \frac{B_1}{B_1 + V_{r2}} \cdot \delta_{\text{fix1}} + \left(\frac{g_2 + g_3\varphi}{\Sigma g} \cdot \frac{V_{r2}}{B_1 + V_{r2}} + \frac{G}{\Sigma g} \right) \cdot \delta_{\text{fix2}} + \frac{g_3(1-\varphi)}{\Sigma g} \cdot \delta_{\text{fix3}} \\
& - p_r \cdot \left(\frac{g_2 + g_3\varphi}{\Sigma g} + \frac{g_3(1-\varphi)}{\Sigma g} \right) + \beta \cdot \left(\frac{g_2 + g_3\varphi}{\Sigma g} \cdot \frac{g_2}{B_1 + V_{r2}} + \frac{g_3}{\Sigma g} \cdot \frac{g_3}{B_3 + V_{r3}} - 1 \right) \\
& + e_m \cdot \left(\frac{g_2 + g_3\varphi}{\Sigma g} \cdot \frac{B_1 R_{m1} + R_{m2}}{B_1 + V_{r2}} + \frac{g_3}{\Sigma g} \cdot \frac{R_{m3}}{B_3 + V_{r3}} \right)
\end{aligned} \tag{11}$$

195 where $\varphi = B_3/(B_3 + V_{r3})$. (11) can be simplified using relationships obtained from mass
196 balance on fixed carbon (with amounts A_2 and A_3) that are such that:

$$197 \quad p_r = -R_{g3}e_g/V_{r3} \tag{12}$$

$$198 \quad \beta = e_g \cdot (-R_{g2} + V_{r2}R_{g3}/V_{r3})/G \tag{13}$$

199

200 Also, the sum of coefficients in front of δ_{fix1} , δ_{fix2} and δ_{fix3} in (11) equals 1 and thus we
201 can simplify notations using the weighted average isotope composition of fixed carbon
202 $\langle \delta_{\text{fix}} \rangle$. Then we obtain:

$$\begin{aligned}
\delta_{\text{grain}} = & \langle \delta_{\text{fix}} \rangle + \frac{e_g}{\Sigma g} \cdot \left(R_{g3} \cdot \frac{g_2 + g_3}{\Sigma g} + \left(R_{g3} \frac{V_{r2}}{V_{r3}} - R_{g2} \right) \cdot \frac{(g_2 + g_3\varphi) \frac{g_2}{B_1 + V_{r2}} + \frac{g_3^2\varphi}{B_3} - \Sigma g}{G} \right) \\
& + \frac{e_m}{\Sigma g} \cdot \left(\left(R_{m1} \cdot \frac{B_1}{B_1 + R_{m1}} + R_{m2} \right) \cdot \frac{g_2 + g_3\varphi}{B_1 + V_{r2}} + R_{m3} \cdot \frac{g_3\varphi}{B_3} \right)
\end{aligned} \tag{14}$$

204 Equation (14) can be abbreviated as follows:

$$205 \quad \delta_{\text{grain}} = \langle \delta_{\text{fix}} \rangle + e_g \cdot \frac{\langle R_g \rangle}{\Sigma g} + e_m \cdot \frac{\langle R_m \rangle}{\Sigma g} \tag{15}$$

206 where $\langle R_g \rangle$ and $\langle R_m \rangle$ represent growth and respiratory sums, corrected for carbon
207 allocation to grains as described by parentheses in (14).

208

209 Of course, $\langle \delta_{\text{fix}} \rangle$ is not very convenient since it is a weighted average and furthermore, it
210 cannot be measured routinely by isotopic online gas exchange in the field. Therefore, it is
211 more useful to use the isotope composition of leaves (vegetative material). Here, we used
212 the isotope composition of leaves at anthesis, where tissues are made of structural
213 material and metabolites (reserves) and are generated up to the end of stage 1/onset of
214 stage 2 (Fig. S2). The weighted average of reserves and structural material produced
215 during stage 1 (full vegetative phase up to anthesis) is given by:

216
$$\delta_{\text{leaf}} = \frac{\delta_{\text{B1}}B_1 + (\delta_{\text{fix1}} - p_s)V_s}{B_1 + V_s} \quad (16)$$

217 which gives, using (7):

218
$$\delta_{\text{leaf}} = \delta_{\text{fix1}} + e_m \cdot \frac{R_{\text{m1}}}{B_1 + R_{\text{m1}}} \theta - p_s \cdot (1 - \theta) \quad (17)$$

219 Where θ is allocation to reserves at stage 1, equal to $B_1/(B_1 + V_s)$. If we assume that δ_{fix1}
 220 $\approx \langle \delta_{\text{fix}} \rangle$, we have:

221
$$\delta_{\text{grain}} - \delta_{\text{leaf}} \approx \frac{\langle R_{\text{m}} \rangle}{\Sigma g} \cdot e_m + \frac{\langle R_{\text{g}} \rangle}{\Sigma g} \cdot e_g - \frac{R_{\text{m1}}}{B_1 + R_{\text{m1}}} \theta \cdot e_m + p_s \cdot (1 - \theta) \quad (18)$$

222 If the respiration use efficiency calculated with respect to net fixed carbon (not gross
 223 assimilation) is denoted as RUE^* , then (18) can be abbreviated using (4) to:

224
$$\delta_{\text{grain}} - \delta_{\text{leaf}} \approx \frac{\text{RUE}^*}{\text{HI}} \cdot e_{\text{mg}} - \frac{R_{\text{m1}}}{B_1 + R_{\text{m1}}} \theta \cdot e_m + p_s \cdot (1 - \theta) \quad (19)$$

225 Where e_{mg} stands for the average fractionation in respiration (growth, maintenance).

226

227 (19) simply says that the isotope composition in grains is the result of carbon partitioning
 228 and as such, can be considered (due to mass balance) as reflecting the carbon material left
 229 behind by the action of fractionations in respiration and structural vegetative biomass. If
 230 the leaf-to-grain difference is denoted as $\Delta\delta$, (19) can be rewritten as:

231
$$\Delta\delta_{\text{corr}} = \Delta\delta - \ell(\theta, p) \approx \frac{\text{RUE}^*}{\text{HI}} \cdot e_{\text{mg}} \quad (20)$$

232 where

233
$$\ell(\theta, p) = -\frac{R_{\text{m1}}}{B_1 + R_{\text{m1}}} \theta \cdot e_m + p_s \cdot (1 - \theta) \text{ and } \Delta\delta = \delta_{\text{grain}} - \delta_{\text{leaf}}$$

234 Also in (19), it should be noted that the order of magnitude of the different terms differs.
 235 Fractionations e_{mg} , e_m and p_s are of a few per mil. The middle term multiplies two
 236 quantities smaller than 1, θ and $R_{\text{m1}}/(B_1 + R_{\text{m1}})$, and thus it is of minor importance. Since
 237 RUE^* is of the order of 0.6-0.8 and HI of about 0.5 in wheat, the first and third terms
 238 predominate numerically in (19). Further information is provided in the [Supplementary](#)
 239 [Text](#) on estimating RUE^* , θ and $R_{\text{m1}}/(B_1 + R_{\text{m1}})$. RUE^* was estimated from biomass
 240 increment and %N using two methods, which gave essentially the same results ([Fig. S3](#)).

241

242 *Estimation of $\delta^{13}\text{C}$ values in leaves.* While measuring the carbon isotope composition in
 243 grains is easy because it just requires sampling upon final harvesting, having $\delta^{13}\text{C}$ values
 244 of leaves at anthesis is much more demanding, both financially and in personnel.
 245 Therefore, we explored the possibility to reconstruct the average $\delta^{13}\text{C}$ value in leaves
 246 from (i) observed agronomic variables via machine learning conducted by multivariate

247 analysis OPLS (Eriksson *et al.*, 2008; Eriksson *et al.*, 2013); (ii) the $\delta^{18}\text{O}$ value observed
248 in grains. These two methods are presented in the [Supplementary Text](#). Method (i)
249 involves multivariate statistics which were performed with Simca® (Umetrics, Sweden).

250

251 *Statistics*

252 Univariate statistics and linear regressions were done in R and with Sigmaplot®. Tests
253 used and significance levels are indicated in figure-e legends.

254 **Results**

255 *Relationship with yield*

256 As expected, there was a negative linear relationship between $\delta^{13}\text{C}_{\text{grain}}$ and yield (Fig. 1),
257 whereby low-yielding plots were up to 3‰ enriched in ^{13}C compared to high-yielding
258 plots. In fact, grain carbon inherits photosynthetically fixed carbon and thus is ^{13}C -
259 enriched when stomatal closure is more pronounced in non-irrigated field plots and in
260 turn restricts isotope discrimination (blue vs. grey points in Fig. 1). This is further
261 illustrated with isolines that showed that the expected generic relationship between yield
262 and $\delta^{13}\text{C}_{\text{grain}}$ was positive, while its slope increased considerably as stomatal closure
263 increased (dashed lines). Interestingly, the relationship between $\delta^{13}\text{C}_{\text{grain}}$ and yield was
264 not influenced by field site showing that wheat cultivars did not differ enormously in
265 their physiological response to environmental conditions.

266

267 *Prediction of $\delta^{13}\text{C}$ in leaves*

268 To extract valuable information on grain properties from $\delta^{13}\text{C}_{\text{grain}}$, we then used the
269 isotopic difference between grain and leaves ($\Delta\delta$), i.e., the apparent grain-to-leaf
270 discrimination. Based on wheat phenology and carbon allocation pattern (see *Theory and*
271 *calculations* in Materials and Methods), we anticipate a generic relationship between $\Delta\delta$,
272 respiratory loss (R_t) and yield (Y) as (equations 18-19):

$$\Delta\delta \approx \frac{R_t}{Y} \cdot e_{\text{mg}} + \ell(\theta, p) \quad (21)$$

273 where e_{mg} is respiratory (growth + maintenance) isotope fractionation and $\ell(\theta, p)$
274 combines the carbon allocation coefficient to reserves (θ) and post-photosynthetic
275 fractionation in structural biomass (straw) production (p). This equation can be rewritten
276 using HI as follows (equation 20):

$$\Delta\delta_{\text{corr}} = \Delta\delta - \ell(\theta, p) \approx \frac{\text{RUE}^*}{\text{HI}} \cdot e_{\text{mg}} \quad (22)$$

277 where RUE^* is the net carbon-based respiration use efficiency. Note this equation is
278 written in such a way to make proportionality apparent between $\Delta\delta_{\text{corr}}$ and RUE^*/HI .
279 However, applying (21) and (22) implies prior knowledge of the $\delta^{13}\text{C}$ value in leaves.
280 This is not something that can be done routinely in the field unlike isotope analysis of
281 grains, which are sampled anyway during harvesting. We thus explored three methods to
282 obtain $\delta^{13}\text{C}_{\text{leaf}}$ (Table 1). In the first dataset (VAR), leaves were sampled and $\delta^{13}\text{C}_{\text{leaf}}$ was
283 thus measured. In the second dataset (BPA), $\delta^{13}\text{C}_{\text{leaf}}$ was reconstructed from agronomic
284 parameters using machine-learning (OPLS multivariate analysis with $\delta^{13}\text{C}$ as the
285 quantitative objective variable). In the third dataset (BVG), $\delta^{13}\text{C}_{\text{leaf}}$ was estimated from
286 the natural ^{18}O abundance in grains (calculations explained in Supplementary Text). This
287 method took advantage of the rather well-conserved $\delta^{18}\text{O}$ difference between leaves and
288 grains, of 2.9‰ (Fig. 5a)

289 Outputs of the multivariate analysis are provided in Fig. 2. The statistical model
290 was trained with dataset 1 (VAR). It was highly significant ($P_{CV-ANOVA} = 1.7 \times 10^{-9}$),
291 robust ($R^2 = 0.68$; $Q^2 = 0.51$) and representative ($Q^2[\text{intercept}] = -0.33$). There was a very
292 strong relationship between predicted and observed $\delta^{13}\text{C}_{\text{leaf}}$ values, with a slope
293 extremely close to unity (0.9998) (Fig. 2a). The role played by the different variables is
294 shown using a volcano plot, representing the variable importance for the projection (VIP)
295 against the loading (pq) (Fig. 2b). In such a representation, the most important drivers
296 have a VIP value above unity and a high loading. $\delta^{13}\text{C}_{\text{leaf}}$ appeared to be most influenced
297 by the previous crop species and N-related traits (red and turquoise points), suggesting a
298 strong effect of nitrogen availability. Multiple linear models are then carried out and
299 similarly, showed the importance of the previous crop species, N-related traits in addition
300 to yield (Fig. 2c). The statistical model was then implemented to calculate $\delta^{13}\text{C}_{\text{leaf}}$ at the
301 second site (BPA). The average was found to be -27.9‰ , with values up to about -25‰
302 and 90% of values being between -27‰ and -29‰ (Fig. 2d).

303 $\delta^{13}\text{C}_{\text{leaf}}$ values computed from $\delta^{18}\text{O}_{\text{grain}}$ at the collective site 3 (BVG) are
304 presented in Fig. S5. The applicability of this method was first checked by comparing
305 observed and computed values at site 1 on different cultivars (Fig. S5b). Average
306 observed and computed $\delta^{13}\text{C}$ values were found to be consistent, by about 1‰, and
307 calculations were thus implemented at site 3.

308

309 *Leaf-to-grain isotope difference*

310 The uncorrected leaf-to-grain $\delta^{13}\text{C}$ difference is shown in Fig. 3. Grains were always
311 found to be ^{13}C -enriched compared to leaves, showing the occurrence of a post-
312 photosynthetic fractionation. Such a fractionation was comprised within 0 and -4‰
313 (negative sign since it was in favour of ^{13}C in grains), except at site 3 where it reached
314 10‰ . As expected from equation 21, there was a negative hyperbolic relationship
315 between $\Delta\delta$ and yield, which fell into the region where the respiratory loss represented
316 about $200 \text{ dt CO}_2 \text{ ha}^{-1}$ (isolines in Fig. 3) at both sites 1 and 2 (VAR, BPA). Also, $\Delta\delta$ was
317 affected by irrigation, with smaller post-photosynthetic fractionation ($\approx 1\text{‰}$) under
318 irrigation and high yield, reflecting the impact of water limitation on isotope allocation to
319 grains. Although in the same graphical region, dataset 3 (BVG) was more scattered due to
320 the much higher imprecision in $\delta^{13}\text{C}_{\text{leaf}}$ estimated from $\delta^{18}\text{O}_{\text{grain}}$.

321 Also, undesirable noise in the relationship between $\Delta\delta$ and yield may have come
322 from reserve remobilisation and variations in biomass allocation. Therefore, we looked at
323 the relationship between corrected $\Delta\delta$ ($\Delta\delta_{\text{corr}}$) and the ratio RUE^*/HI (equation 22). At
324 both sites (VAR and BPA), $\Delta\delta_{\text{corr}}$ fell within a narrow region delimited by isolines
325 obtained with different respiratory isotope fractionations (from 2.5 to 4‰) (Fig. 4a-b). It
326 formed a significant linear relationship with RUE^*/HI (dash-dotted black line). This
327 relationship was not examined using dataset 3 (BVG) since biomass, %N and growth data

328 were not available and thus RUE^* and $\Delta\delta_{\text{corr}}$ could not be estimated. Interestingly, data
329 points obtained under irrigated and non-irrigated conditions partly overlapped and were
330 in the same region of the graph, with no significant isotope offset, and thus appeared to
331 be on the same relationship.

332

333 *Possible links to grain properties*

334 Under our conditions, the relationship between $\Delta\delta_{\text{corr}}$ and RUE^*/HI was probably not
335 driven by differences in grain specific weight (GSW, mass per grain volume) since no
336 difference was found between conditions in GSW (Fig. 4c and 4f). It suggests that
337 changes in carbon allocation reflected by RUE^* and HI were not associated with different
338 grain size but rather changes in total grain set per plant. There were differences in straw
339 or grain nitrogen (%N) across conditions (Fig. 4d, e, g and h). Since the nitrogen content
340 was also a determinant of $\delta^{13}\text{C}_{\text{leaf}}$ (see above), N assimilation and remobilisation thus
341 appeared to be an important parameter in $\Delta\delta_{\text{corr}}$ typically via both photosynthetic capacity
342 and grain metabolism.

343 **Discussion**

344 Our results show that the apparent isotope fractionation between leaves (at anthesis) and
345 grain (at maturity), $\Delta\delta_{\text{corr}}$, correlates to parameters associated with respiration use
346 efficiency (RUE^*) and harvest index (HI) in wheat. In addition to giving information on
347 isotope biochemistry beyond photosynthesis (i.e. on grain production itself), it suggests
348 that $\Delta\delta_{\text{corr}}$ is a potentially useful marker to trace carbon partitioning carbon utilisation. In
349 fact, the RUE^* -to-HI ratio reflects C allocation: the larger the ratio, the higher the
350 respiratory loss and/or the lower the grain relative biomass fraction. In what follows, we
351 address this point by discussing causes of the leaf-to-grain isotope fractionation and
352 possible limitations in using $\Delta\delta_{\text{corr}}$.

353

354 *Origin of the relationship between grain isotope fractionation $\Delta\delta_{\text{corr}}$ and RUE^*/HI*

355 The relationship between $\Delta\delta_{\text{corr}}$ and RUE^*/HI (Fig. 4) is a consequence of respiratory loss
356 and biomass production, which are accompanied by isotope effects (represented by
357 fractionation factors e_{mg} and p in equations). In practice, this suggests that highly
358 performing wheat plants are naturally less ^{13}C -enriched due to a lower relative impact of
359 respiration and higher commitment to biomass synthesis, thus minimizing apparent, post-
360 photosynthetic isotope fractionations.

361 The proportionally lower respiration in highly performing wheat lines has
362 effectively been observed experimentally (McCullough & Hunt, 1989). Of course, our
363 interpretation of variations in $\Delta\delta_{\text{corr}}$ is somewhat simplified since parameters other than
364 e_{mg} and p participate in equations (such as partitioning to reserves, θ) and furthermore,
365 equations (18-22) are a simplification (i.e., require approximations, see also discussion
366 below). This probably explains part of the noise present in Fig. 4, along with variation in
367 e_{mg} itself. Still, it is striking that nearly all of the datapoints are within the graphical
368 region defined by $e_{\text{mg}} = 2$ and 4‰ (Fig. 4).

369 The fact that carbon partitioning translates into changes in $\Delta\delta_{\text{corr}}$ is also likely
370 associated with changes in nitrogen partitioning: First, $\delta^{13}\text{C}_{\text{leaf}}$ was found to depend on
371 leaf N content and availability (Fig. 2); Second, some changes were observed in grain or
372 straw N content between conditions (Fig. 4); Third, nitrogen availability has a well-
373 known effect on carbon partitioning (including the shoot-root ratio) and respiration in
374 wheat (Pearman *et al.*, 1981; Cox *et al.*, 1986; Hay, 1995; Sinclair, 1998; Kichey *et al.*,
375 2007; Allard *et al.*, 2013). In our case, wheat plots were fertilised at relatively similar
376 levels (*c.* 200 kg ha⁻¹) which are commonly used under ordinary culture conditions (200
377 kg ha⁻¹ is the average value compiled by the FAO, www.fao.org). In other words, $\Delta\delta_{\text{corr}}$
378 would probably appear to be less strongly related to RUE^*/HI if fertilisation regimes had
379 been extremely different between sites or plots (for example, no fertilisation at all and
380 more than 250 kg N ha⁻¹).

381 Importantly, the relationship between $\Delta\delta_{\text{corr}}$, RUE*/HI did not depend much on
382 water relations. In effect, while the response of $\delta^{13}\text{C}_{\text{grain}}$ to yield was mostly driven by
383 water availability and thus conductance and thus photosynthetic conditions as in (Merah
384 *et al.*, 2001a; Merah *et al.*, 2001b) (Fig. 1), irrigation had a rather small effect on the
385 relationship between $\Delta\delta_{\text{corr}}$ and RUE*/HI, all data points being apparently on the same
386 line (Fig. 4). For example, under oceanic climate (site VAR), the average offset between
387 irrigated and non-irrigated conditions was *c.* 0.7‰ only (Fig. 4a) and was statistically
388 insignificant. In other words, although non-irrigated conditions impacted on overall
389 allocation to grains and thus the harvest index, there was little effect on fractionation
390 factors and as a result, datapoints followed the same relationship as that found under
391 irrigated conditions. Accordingly, drought conditions have effectively been shown to
392 have little effect on metabolic discriminations, in particular in respiration in other crops
393 (Duranceau *et al.*, 1999; Ghashghaie *et al.*, 2001).

394

395 *Pros and cons of the theoretical background used here*

396 The theoretical background used here to obtain a relationship between $\Delta\delta_{\text{corr}}$ and
397 RUE*/HI (equations 20 and 22) implied several approximations. We assumed that
398 reserves accumulated during first stages are remobilised at later stage with minimal left
399 overs of unused carbon reserves ($\Delta B = 0$ in equation 4). This assumption is likely not
400 critical since wheat straw is effectively very poor in non-structural carbohydrates (and
401 protein) [for a recent overview, see (Wang *et al.*, 2020)] showing very efficient
402 remobilisation. Also, isotopic labelling has shown that up to 94% of available protein and
403 water-soluble carbohydrates are effectively used for grain filling (Gebbing *et al.*, 1999).
404 We further assumed that leaves sampled at anthesis were representative of fixed carbon
405 (accounting for biomass and reserves deposition, equation 16). This assumption was
406 driven by technical imperatives because the true value of the weighted average of fixed
407 carbon, $\langle\delta_{\text{fix}}\rangle$, is not accessible. It is probably not too critical since reserves accumulated
408 during the vegetative stage have a high contribution to grain carbon, of up to 50%
409 (Schnyder, 1993; Gent, 1994; Gebbing *et al.*, 1999). In addition, if photosynthetic
410 properties of leaves were to vary significantly (with typically lower c_i/c_a during
411 summertime), it would mean that the isotope composition of fixed carbon up to anthesis
412 would be slightly ^{13}C -depleted compared to $\langle\delta_{\text{fix}}\rangle$. This isotopic difference would add in
413 the intercept of the relationship in (19) and Fig. 4, not in the slope, and therefore the
414 correlation between $\Delta\delta_{\text{corr}}$ and RUE*/HI would remain valid, with some noise due to
415 variations in $\langle\delta_{\text{fix}}\rangle$. In other words, our assumption $\langle\delta_{\text{fix}}\rangle \approx \delta_{\text{fix}1}$ probably explains some of
416 the scattering but cannot explain the linear relationship in Fig. 4. It is also possible that
417 the small offset between irrigated and non-irrigated conditions (blue vs. grey points in
418 Fig. 4) was explained by this effect. That said, the ^{13}C -enriching effect of dry conditions
419 in summer must be compensated for by the ^{13}C -depleting effect of refixation of CO_2

420 respired by glumes, which has a non-negligible contribution to grain organic matter
421 (Araus *et al.*, 1993; Gebbing & Schnyder, 2001). Taken as a whole, variations in overall
422 photosynthetic isotopic input are probably not huge and cannot alter the relationship
423 described here.

424 We also recognise that although convenient, equation (22) is an abbreviated
425 formulation of the full expression describing post-photosynthetic processes (compare
426 equations 14 and 15 and compare 15 and 19). Nevertheless, the abbreviated final
427 equation (22) allows application with readily accessible variables in the field. Taken as a
428 whole, a generic respiratory fractionation (here denoted as e_{mg}), which encapsulates
429 weighted maintenance and growth respiration parameters, seems to be sufficient to model
430 $\Delta\delta_{corr}$. In addition, the apparent value of e_{mg} adapted to linear fitting (2.5 to 4‰) (Fig. 4,
431 coloured lines) indicates that at the plant scale (above-ground organs), respiratory
432 metabolism yields ^{13}C -depleted CO_2 . The generation of ^{13}C -depleted CO_2 is a general
433 feature in heterotrophic organs of C_3 plants (Klumpp *et al.*, 2005; Bathellier *et al.*, 2009;
434 Ghashghaie & Badeck, 2014; Bathellier *et al.*, 2017).

435

436 *Potential utilisation of the relationship between $\Delta\delta_{corr}$ and RUE^*/HI*

437 The observed robustness of the relationship between $\Delta\delta_{corr}$ and RUE^*/HI (with respect to
438 water availability and sites) is essential to envisage potential applications. In fact, having
439 low values of the ratio RUE^*/HI reflect minimal respiratory losses (low RUE^*) and/or
440 good allocation to grains (high HI), and is thus beneficial. That is, selecting for low $\Delta\delta_{corr}$
441 values could thus help finding cultivars with better performance in carbon partitioning to
442 grains. This would be of prime interest for current strategies to get higher yield in wheat,
443 which include an increase in HI and minimization of carbon losses by respiration
444 (Reynolds *et al.*, 2012). Also, HI appears to condition responsiveness to high CO_2
445 (Aranjuelo *et al.*, 2013) and is thus of importance under current conditions of global
446 change. In the recent past, considerable efforts have been devoted to biometrics, QTL or
447 GWAS to identify key markers associated with yield or harvest index (Reynolds *et al.*,
448 2017; Quintero *et al.*, 2018; Pradhan *et al.*, 2019; Rivera-Amado *et al.*, 2019; Porker *et al.*,
449 2020). In addition, domesticated high-yielding dwarf varieties with changed carbon
450 (as well as nitrogen and sulphur) allocation, show changes in grain specific weight
451 (Casebow *et al.*, 2016) although the trade-off between grain number and specific weight
452 seems to depend on environmental conditions (Quintero *et al.*, 2018).

453 Future studies are warranted to determine whether the isotope difference $\Delta\delta_{corr}$
454 can be used as an advantageous trait for breeding, since (i) it encapsulates a complex
455 carbon allocation parameter (RUE^*/HI) that is not accessible otherwise, and (ii) the
456 $\Delta\delta_{corr}$ - RUE^*/HI relationship changes minimally with growth conditions. When $\delta^{13}\text{C}_{leaf}$ at
457 anthesis is not available to compute $\Delta\delta_{corr}$, our study further suggests it can be estimated
458 with multivariate analysis or $\delta^{18}\text{O}$. It is now well-accepted that there is good heritability

459 of $^{12}\text{C}/^{13}\text{C}$ isotope composition not only in leaves but also in grains (Merah *et al.*, 2001a).
460 Taken as a whole, we suggest that interesting allocation properties can be accessed via
461 $\Delta\delta_{\text{corr}}$, which gives direct information on events during grain filling and thus may help
462 isotope-based implementation of genotype selection.

463 **Acknowledgments**

464 This work was supported by the *Région Pays de la Loire* and *Angers Loire Métropole* via
465 the program *Connect Talent* Isoseed and the University of Angers via a PhD grant to
466 J.B.D. The authors also thank the financial support of the *Groupement Interprofessionnel*
467 *des Semences et Plantes* via the project 2012K "Identification of drought tolerance traits in
468 winter wheat and constitution of tools adapted to their evaluation" of the scheme *Fonds*
469 *de Soutien à l'Obtention Végétale* (field trials BPV and VAR). The field trial BPA was
470 carried out jointly by PIA-ANR via the project BreedWheat (ANR-10-BTBR-003). The
471 authors thank Hilary Stuart-Williams (ANU Isotope Facility) for $^{18}\text{O}/^{16}\text{O}$ isotope
472 analyses.

473

474 **Author Contributions**

475 J.C.D., E.O., V.L., C.Z., L.D., C.B., P.L., J.D., and T.M. conceived the field experiment,
476 organised wheat cultivation field trials and sampling. K.B. performed agronomic
477 measurements. C.A. prepared samples for the isotopic analysis. M. LS. Carried out
478 isotopic $^{12}\text{C}/^{13}\text{C}$ analyses. J.B.D. and G.T. conceived the concept and developed the
479 scenarios associated with $\Delta\delta$ in grains. J.L. and A.M.L. checked the validity of isotopic
480 analyses. G.T. wrote the paper. J.B.D. managed data storing and availability on the
481 INRAe server. All authors read or contributed to the final version of the paper.

482

483 **Competing Interest Statement:** The authors declare no conflict of interest.

References

- Allard V, Martre P, Le Gouis J. 2013. Genetic variability in biomass allocation to roots in wheat is mainly related to crop tillering dynamics and nitrogen status. *European Journal of Agronomy* **46**: 68-76.
- Aranjuelo I, Sanz-Sáez Á, Jauregui I, Irigoyen JJ, Araus JL, Sánchez-Díaz M, Erice G. 2013. Harvest index, a parameter conditioning responsiveness of wheat plants to elevated CO₂. *Journal of experimental botany* **64**: 1879-1892.
- Araus JL, Brown HR, Febrero A, Bort J, Serret MD. 1993. Ear photosynthesis, carbon isotope discrimination and the contribution of respiratory CO₂ to differences in grain mass in durum wheat. *Plant Cell and Environment* **16**: 383-392.
- Badeck FW, Tcherkez G, Nogues S, Piel C, Ghashghaie J. 2005. Post-photosynthetic fractionation of stable carbon isotopes between plant organs—a widespread phenomenon. *Rapid Communications in Mass Spectrometry* **19**: 1381-1391.
- Bathellier C, Badeck F-W, Ghashghaie J 2017. Carbon isotope fractionation in plant respiration. In: Tcherkez G, Ghashghaie J eds. *Plant respiration: Metabolic fluxes and carbon balance*. Berlin: Springer, 43-68.
- Bathellier C, Tcherkez G, Bligny R, Gout E, Cornic G, Ghashghaie J. 2009. Metabolic origin of the $\delta^{13}\text{C}$ of respired CO₂ in roots of *Phaseolus vulgaris*. *New Phytologist* **181**: 387-399.
- Casebow R, Hadley C, Uppal R, Addisu M, Loddo S, Kowalski A, Griffiths S, Gooding M. 2016. Reduced height (*Rht*) alleles affect wheat grain quality. *Plos one* **11**: e0156056.
- Cernusak LA, Tcherkez G, Keitel C, Cornwell WK, Santiago LS, Knohl A, Barbour MM, Williams DG, Reich PB, Ellsworth DS. 2009. Why are non-photosynthetic tissues generally ¹³C enriched compared with leaves in C₃ plants? Review and synthesis of current hypotheses. *Functional Plant Biology* **36**: 199-213.
- Condon A, Farquhar G, Richards R. 1990. Genotypic Variation in Carbon Isotope Discrimination and Transpiration Efficiency in Wheat. Leaf Gas Exchange and Whole Plant Studies. *Functional Plant Biology* **17**: 9-22.
- Condon A, Richards R, Farquhar G. 1987. Carbon Isotope Discrimination is Positively Correlated with Grain Yield and Dry Matter Production in Field-Grown Wheat. *Crop Science* **27**: 996-1001.
- Condon AG, Richards R, Rebetzke G, Farquhar G. 2004. Breeding for high water-use efficiency. *Journal of Experimental Botany* **55**: 2447-2460.
- Cox MC, Qualset CO, Rains DW. 1986. Genetic variation for nitrogen assimilation and translocation in wheat. III. Nitrogen translocation in relation to grain yield and protein. *Crop Science* **26**: 737-740.
- Duranceau M, Ghashghaie J, Badeck F, Deleens E, Cornic G. 1999. $\delta^{13}\text{C}$ of CO₂ respired in the dark in relation to $\delta^{13}\text{C}$ of leaf carbohydrates in *Phaseolus vulgaris* L. under progressive drought. *Plant Cell and Environment* **22**: 515-523.
- Eriksson L, Byrne T, Johansson E, Trygg J, Vikström C. 2013. *Multi-and megavariable data analysis basic principles and applications*. Malmö: Umetrics Academy.
- Eriksson L, Trygg J, Wold S. 2008. CV-ANOVA for significance testing of PLS and OPLS® models. *Journal of Chemometrics: A Journal of the Chemometrics Society* **22**: 594-600.
- Farquhar GD, Ehleringer JR, Hubick KT. 1989. Carbon isotope discrimination and photosynthesis. *Annual review of plant biology* **40**: 503-537.
- Gebbing T, Schnyder H. 2001. ¹³C labeling kinetics of sucrose in glumes indicates significant re-fixation of respiratory CO₂ in the wheat ear. *Functional Plant Biology* **28**: 1047-1053.

- Gebbing T, Schnyder H, Kühbauch W. 1999.** The utilization of pre-anthesis reserves in grain filling of wheat. Assessment by steady-state $^{13}\text{CO}_2/^{12}\text{CO}_2$ labelling. *Plant Cell and Environment* **22**: 851-858.
- Gent M. 1994.** Photosynthate reserves during grain filling in winter wheat. *Agronomy Journal* **86**: 159-167.
- Ghashghaie J, Badeck FW. 2014.** Opposite carbon isotope discrimination during dark respiration in leaves versus roots—a review. *New Phytologist* **201**: 751-769.
- Ghashghaie J, Duranceau M, Badeck FW, Cornic G, Adeline MT, Deleens E. 2001.** $\delta^{13}\text{C}$ of CO_2 respired in the dark in relation to $\delta^{13}\text{C}$ of leaf metabolites: comparison between *Nicotiana sylvestris* and *Helianthus annuus* under drought. *Plant Cell and Environment* **24**: 505-515.
- Gilbert A, Robins RJ, Remaud GS, Tcherkez GG. 2012.** Intramolecular ^{13}C pattern in hexoses from autotrophic and heterotrophic C_3 plant tissues. *Proceedings of the National Academy of Sciences* **109**: 18204-18209.
- Gleixner G, Danier HJ, Werner RA, Schmidt HL. 1993.** Correlations between the ^{13}C content of primary and secondary plant products in different cell compartments and that in decomposing basidiomycetes. *Plant physiology* **102**: 1287-1297.
- Hay RKM. 1995.** Harvest index: a review of its use in plant breeding and crop physiology. *Annals of Applied Biology* **126**: 197-216.
- Kelly S, Heaton K, Hoogewerff J. 2005.** Tracing the geographical origin of food: The application of multi-element and multi-isotope analysis. *Trends in Food Science Technology* **16**: 555-567.
- Kichey T, Hirel B, Heumez E, Dubois F, Le Gouis J. 2007.** In winter wheat (*Triticum aestivum* L.), post-anthesis nitrogen uptake and remobilisation to the grain correlates with agronomic traits and nitrogen physiological markers. *Field Crops Research* **102**: 22-32.
- Klump K, Schäufele R, Löttscher M, Lattanzi FA, Feneis W, Schnyder H. 2005.** C-isotope composition of CO_2 respired by shoots and roots: fractionation during dark respiration? *Plant Cell and Environment* **28**: 241-250.
- Kodina L. 2010.** Carbon isotope fractionation in various forms of biogenic organic matter: I. Partitioning of carbon isotopes between the main polymers of higher plant biomass. *Geochemistry International* **48**: 1157-1165.
- Ma WT, Tcherkez G, Wang XM, Schäufele R, Schnyder H, Yang Y, Gong XY. 2020.** Accounting for mesophyll conductance substantially improves ^{13}C -based estimates of intrinsic water-use efficiency. *New Phytologist* **229**: 1326-1338.
- McCullough DE, Hunt LA. 1989.** Respiration and dry matter accumulation around the time of anthesis in field stands of winter wheat (*Triticum aestivum*). *Annals of Botany* **63**: 321-329.
- Merah O, Deléens E, Al Hakimi A, Monneveux P. 2001a.** Carbon isotope discrimination and grain yield variations among tetraploid wheat species cultivated under contrasting precipitation regimes. *Journal of Agronomy and Crop Science* **186**: 129-134.
- Merah O, Deléens E, Monneveux P. 2001b.** Relationships between carbon isotope discrimination, dry matter production, and harvest index in durum wheat. *Journal of Plant Physiology* **158**: 723-729.
- Merah O, Deléens E, Teulat B, Monneveux P. 2002.** Association between yield and carbon isotope discrimination value in different organs of durum wheat under drought. *Journal of Agronomy and Crop Science* **188**: 426-434.
- Pearman I, Thomas SM, Thorne GN. 1981.** Dark respiration of several varieties of winter wheat given different amounts of nitrogen fertilizer. *Annals of Botany* **47**: 535-546.
- Porker K, Straight M, Hunt JR. 2020.** Evaluation of $G \times E \times M$ interactions to increase harvest index and yield of early sown wheat. *Frontiers in Plant Science* **11**: 994.

- Pradhan S, Babar MA, Robbins K, Bai G, Mason RE, Khan J, Shahi D, Avci M, Guo J, Maksud Hossain M, et al. 2019.** Understanding the genetic basis of spike fertility to improve grain number, harvest index, and grain yield in wheat under high temperature stress environments. *Frontiers in Plant Science* **10**: 1481.
- Quintero A, Molero G, Reynolds MP, Calderini DF. 2018.** Trade-off between grain weight and grain number in wheat depends on GxE interaction: A case study of an elite CIMMYT panel (CIMCOG). *European Journal of Agronomy* **92**: 17-29.
- Remaud GS, Akoka S. 2017.** A review of flavors authentication by position-specific isotope analysis by nuclear magnetic resonance spectrometry: the example of vanillin. *Flavour and Fragrance Journal* **32**: 77-84.
- Reynolds M, Foulkes J, Furbank R, Griffiths S, King J, Murchie E, Parry M, Slafer G. 2012.** Achieving yield gains in wheat. *Plant, Cell and Environment* **35**: 1799-1823.
- Reynolds MP, Pask AJD, Hoppitt WJE, Sonder K, Sukumaran S, Molero G, Pierre CS, Payne T, Singh RP, Braun HJ, et al. 2017.** Strategic crossing of biomass and harvest index—source and sink—achieves genetic gains in wheat. *Euphytica* **213**: 257.
- Rivera-Amado C, Trujillo-Negrellos E, Molero G, Reynolds MP, Sylvester-Bradley R, Foulkes MJ. 2019.** Optimizing dry-matter partitioning for increased spike growth, grain number and harvest index in spring wheat. *Field Crops Research* **240**: 154-167.
- Sanchez-Bragado R, Newcomb M, Chairi F, Condorelli GE, Ward RW, White JW, Maccaferri M, Tuberosa R, Araus JL, Serret Molins MD. 2020.** Carbon Isotope Composition and the NDVI as Phenotyping Approaches for Drought Adaptation in Durum Wheat: Beyond Trait Selection. *Journal of Agronomy* **10**: 1679.
- Santesteban L, Miranda C, Barbarin I, Royo J. 2015.** Application of the measurement of the natural abundance of stable isotopes in viticulture: a review. *Australian journal of grape wine research* **21**: 157-167.
- Schmidt H, Gleixner G 1998.** Carbon isotope effects on key reactions in plant metabolism and ¹³C-patterns in natural compounds. In: Griffiths H ed. *Stable Isotopes: Integration of biological, ecological geochemical processes*. Oxon, UK: Garland Science (Taylor and Francis), 13-25.
- Schnyder H. 1993.** The role of carbohydrate storage and redistribution in the source-sink relations of wheat and barley during grain filling - a review. *New Phytologist* **123**: 233-245.
- Sinclair TR. 1998.** Historical changes in harvest index and crop nitrogen accumulation. *Crop Science* **38**: 638-643.
- Touzy G, Rincent R, Bogard M, Lafarge S, Dubreuil P, Mini A, Deswarte J-C, Beauchêne K, Le Gouis J, Praud S. 2019.** Using environmental clustering to identify specific drought tolerance QTLs in bread wheat (*T. aestivum* L.). *Theoretical and Applied Genetics* **132**: 2859-2880.
- Wang X, Yang Z, Liu X, Huang G, Xiao W, Han L. 2020.** The composition characteristics of different crop straw types and their multivariate analysis and comparison. *Waste Management* **110**: 87-97.

Table 1. Summary of agronomic properties of cultivation sites. Average temperature and precipitations are associated with the growing and maturation season (March-June). Plant density was within 200-300 m⁻² in all parcels. Sowing date was Nov 1st (VAR), 17th (BPA) and at various dates in the second half of October (BVG).

Abbr.	Name	Climate	Av. temp. (°C)	Prec. (mm)	Previous crop	Fert. (kgN/ha)	No. of parcels	No. of cultivars	Isotopes
Field site 1									
VAR	Saint Pierre d'Amilly (France)	Oceanic	13.4	283	Rapeseed or pea	200	87	8	$\delta^{13}\text{C}$, $\delta^{18}\text{O}$ measured in both grains and leaves
Field site 2									
BPA	Gréoux les Bains (France)	Supramediterranean	14.4	156	Sunflower	210	379	70	$\delta^{13}\text{C}$ measured in grains, $\delta^{13}\text{C}$ in leaves simulated by machine learning
Collective field site 3									
BVG	Various (France, Hungary)	Various (oceanic to mediterranean)	11.4-13.9	180-250	Sunflower, wheat or pea	180-220	178	38	$\delta^{13}\text{C}$ and $\delta^{18}\text{O}$ in grains; $\delta^{13}\text{C}$ in leaves reconstructed from $\delta^{18}\text{O}$ in grains

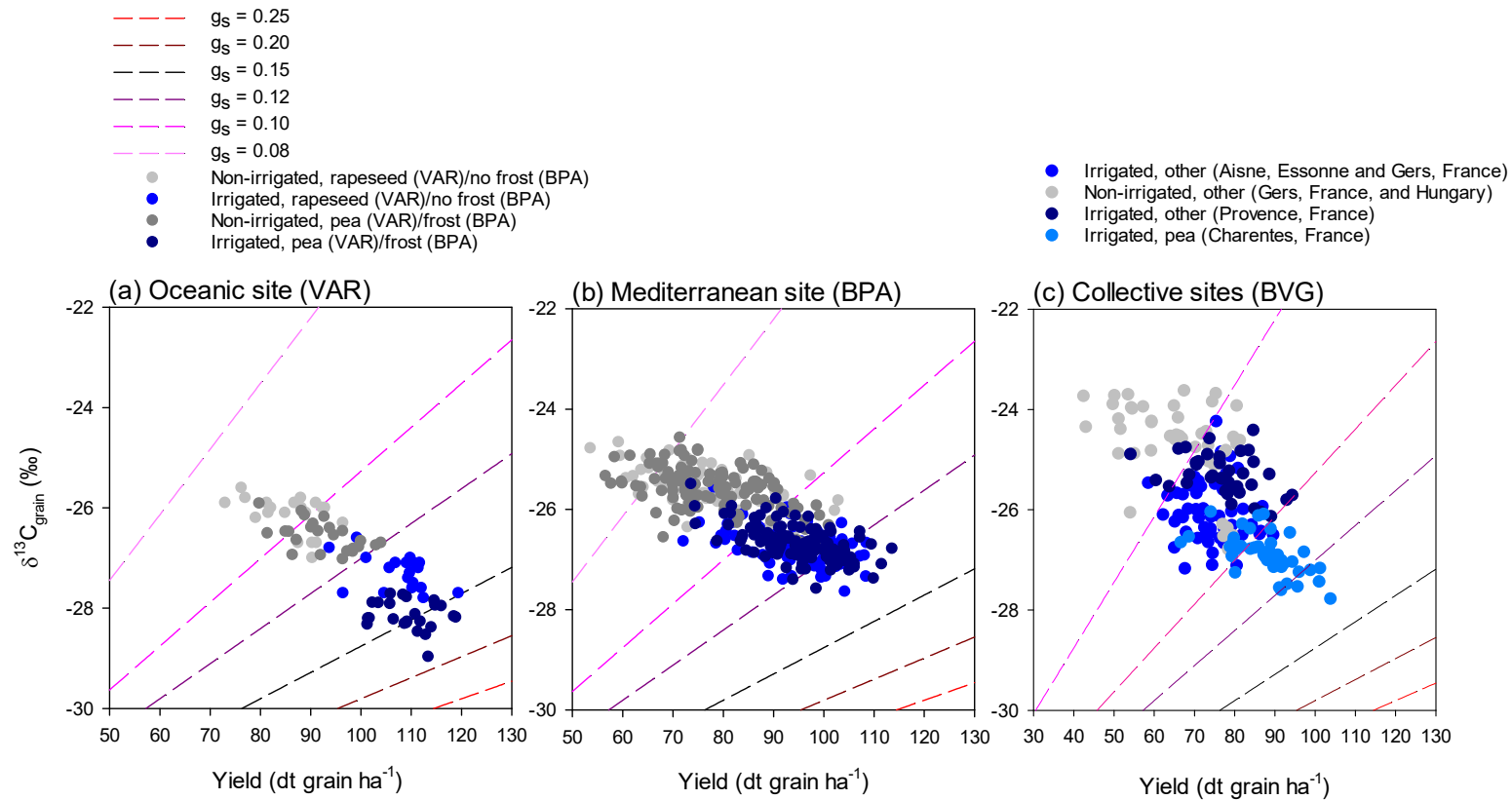


Fig. 1. Carbon isotope composition in wheat grains, expressed in absolute V-PDB scale as a $\delta^{13}\text{C}$. Wheat was cultivated under oceanic (VAR, a), Mediterranean (BPA, b) climatic conditions or across different sites (BVG, c). Wheat was grown under irrigated or non-irrigated plots, used previously to grow pea or other plants, and experiencing occasional frost or not (BPA). $\delta^{13}\text{C}$ values are plotted against yield, in decitons grain (at standard 15% humidity) per hectare. Isolines stand for expected linear relationship using the simplified photosynthetic model of isotope fractionation, with different values of average stomatal conductance g_s (in $\text{mol m}^{-2} \text{s}^{-1}$) (equation S11 in [Supplementary Material](#)). Note that all data points are not on the same isoline due to variations in average stomatal conductance across growth conditions, however, the relationship between $\delta^{13}\text{C}$ and yield is similar across sites.

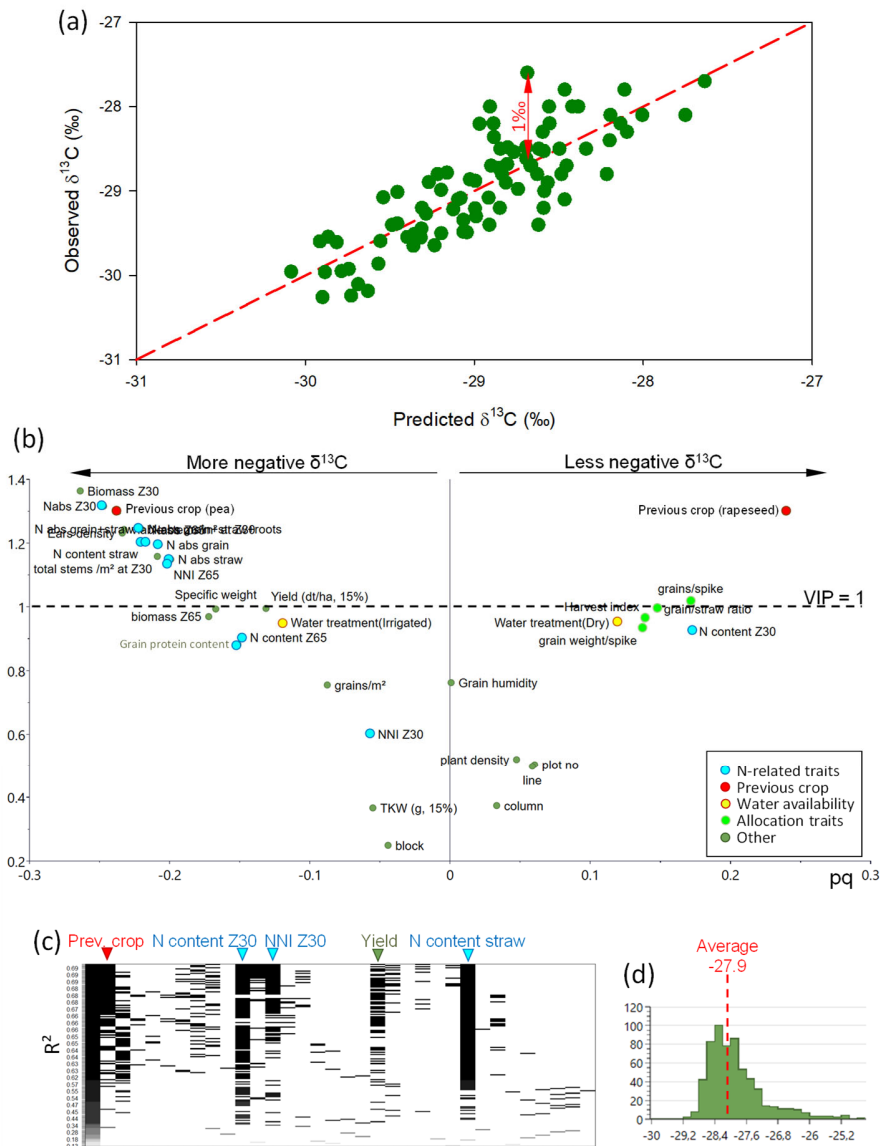


Fig. 2. Statistical analysis of $\delta^{13}\text{C}$ in leaves using dataset 1 (VAR) (a-c) and application of the multivariate model to dataset 2 (BPA) to predict $\delta^{13}\text{C}$ values (d). (a) Output of the OPLS model showing the correlation between predicted and observed $\delta^{13}\text{C}$ values. The maximum error made by the model is 1‰ (red arrow). Dashed line, regression line ($y = 0.9998x - 0.00518$; $P < 0.001$; $R^2 = 0.68$). (b) Volcano plot showing the most important variables using the loading value (pq, x-axis) against the variable importance for the projection (VIP, y-axis). Different colours are used to distinguish the types of agronomic variables (see legend). The dashed horizontal line stands for the usual threshold value used in multivariate analyses (VIP = 1). (c) Output of multiple linear models (sampling of 7 variables amongst 33 variables) showing the distribution of R^2 values. The four best variables are the previous crop, the N content in straw and in leaves at stage Z30 and the nitrogen nutrition index (NNI) at Z30 (arrowheads). The left lane corresponds to the grey scale. (d) Spectrum of predicted $\delta^{13}\text{C}$ values in leaves for the Mediterranean site (BPA) using a frequency graph, where the average value was found to be -27.9 ‰ (red).

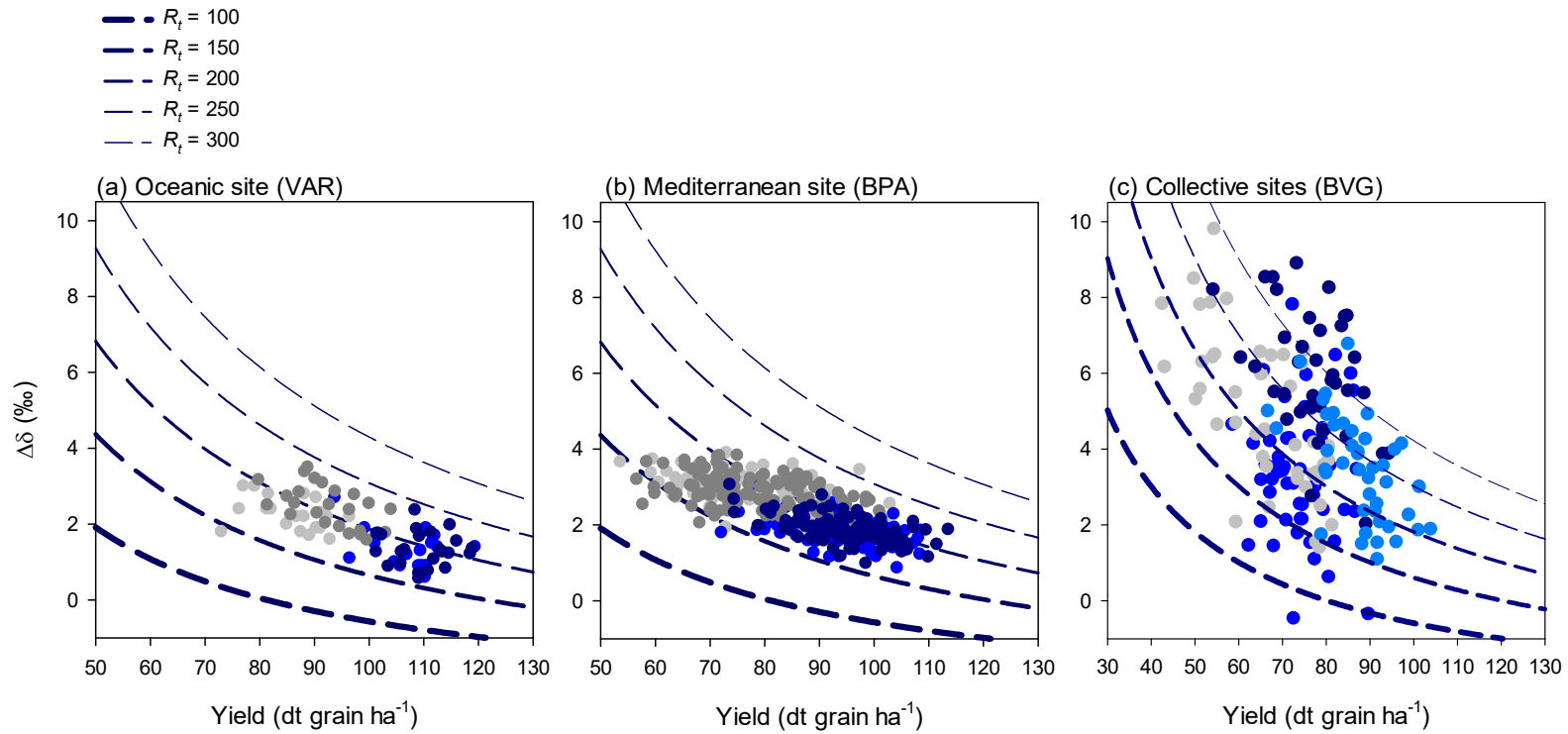


Fig. 3. Uncorrected $\delta^{13}\text{C}$ difference between grains and leaves, $\Delta\delta$. Same legend as in Fig. 1. $\delta^{13}\text{C}$ value in grains was measured and the $\delta^{13}\text{C}$ value in leaves was either measured or estimated from multivariate modelling or observed $\delta^{18}\text{O}_{\text{grain}}$ (Table 1). Isolines represent the reciprocal relationship with yield ($Y = \Sigma g$) and total respiration (R_t) (equation 21), with $p = -3\text{‰}$, $e_{\text{mg}} = 3\text{‰}$ and different values of total respiration R_t (in decitons CO_2 per hectare).

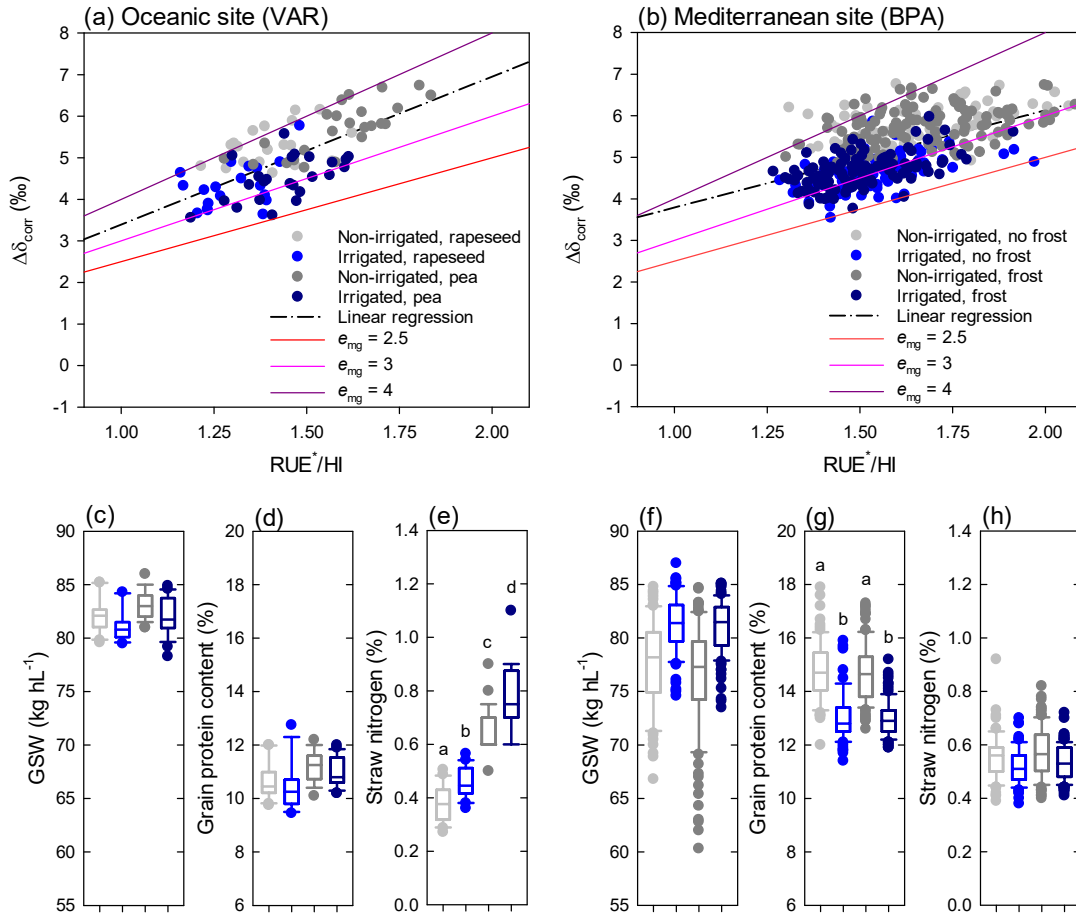


Fig. 4. Corrected isotope leaf-grain difference $\Delta\delta_{\text{corr}}$ and physiological properties of grain and straw in wheat cultivated at sites 1 (VAR) and 2 (BPA) (same symbols as in Fig. 1). (a,b) $\Delta\delta_{\text{corr}}$ plotted against estimated respiration use efficiency-to-harvest index ratio, RUE^*/HI . Colored lines stand for isolines (expected proportionality relationships) with respiratory fractionation e_{mg} equal to 2.5, 3 or 4‰. Dashed-dotted line, linear regression, which is significant ($P < 0.0001$) with $R^2 = 0.48$ (a) and 0.61 (b). (c,f) Grain specific weight, in kilograms per hectoliter. (d,g) Grain protein content, in % weight. (e,h) Nitrogen elemental content in straw. Letters stand for statistical classes (ANOVA, $P < 0.01$).